

## A NEW ENERGY CONTROLLED CURRENT SOURCE INVERTER FED INDUCTION MOTOR DRIVE

Gabor Fekete

University of Miskolc, Department of Electrical and Electronic Engineering, 3515 Miskolc-Egyetemvaros

tel.: ++ 36 46 566 111 /12 17; e-mail: elkfegab@gold.uni-miskolc.hu

**Abstract.** A new induction motor drive control strategy is introduced for current source inverter. The so-called energy model is used. The energy control diagram is presented that is the base of the strategy. Speed or torque control can be realised without measurement or calculation of mechanical speed. Laboratory experimental results are also presented.

**Keywords:** Adjustable speed drives, Sensorless control, Current-based energy control, Contact energy control diagram, Standardised control strategy for inverter-fed drives, Shaft-frequency seeking and tracking logic, Low speed control.

Košice  
Slovak Republic  
2000

### 1. INTRODUCTION

High performance, Reliable induction motor drives can be realised by controlled current or voltage source inverters. Therefore induction motors are more and more popular nowadays. Inverter-fed squirrel-cage induction motors can be used in dangerous environment also, for example in mining and in chemical and oil industry. The application of sensorless drives is especially advantageous in the above-mentioned risky environment. The control strategy introduced in these paper gives excellent results without calculation or measurement of rotor speed.

### 2. ENERGY MODEL OF INDUCTION MACHINE

The generally used induction machine model consists of resistances and inductance. A modified "Energy Model" is used during the research work, where only the stator resistance is taken into consideration with its original value. The motor remainder part is represented by the  $L^*$  and  $R^*$  equivalent elements, as it is shown in Fig. 1. The vectors of stator voltage space vector  $\bar{U}$ , the stator current space vector  $\bar{I}$ , and the stator resistance  $R$  are derived continuously from the motor. Therefore the flux  $\bar{\phi}$  and stator current  $\bar{I}$  space vectors are equal to the actual motor values, that means that the used main field and leakage values are errorless, and the equivalent  $L^*$  and  $R^*$  values are not calculated. The electromagnetic energy  $E_0$  inside the motor represents the energy of the magnetic wave field produced by voltage or current compulsion and is considered as a potential energy. Reserving the compulsion of magnetic wave field, the rotor installed into the magnetic wave field produces effective watt energy due to the  $f_2$  rotor frequency. This energy is considered also as potential energy and is known as the shaft torque. The  $T$  torque and the magnetic energy  $E_0$  are considered as the real and imaginary components of the  $\bar{E}$  contact energy space vector. The  $\bar{E}$  vector

coincides with the  $\bar{I}$  current vector and can be determined from the relation between  $\bar{\phi}$  and  $\bar{I}$ . The flux  $\bar{\phi}$  and the current  $\bar{I}$  are directed fields. The directed field derives from the mutual effect between the material field and the material-free field (vacuum field). The scale of setting in direction gives the field intensity of the directed field. The simplified induction machine construction model and the space vectors in synchronous reference frame are shown in Fig. 2. Motor mode is taken into consideration and the energy model is used.

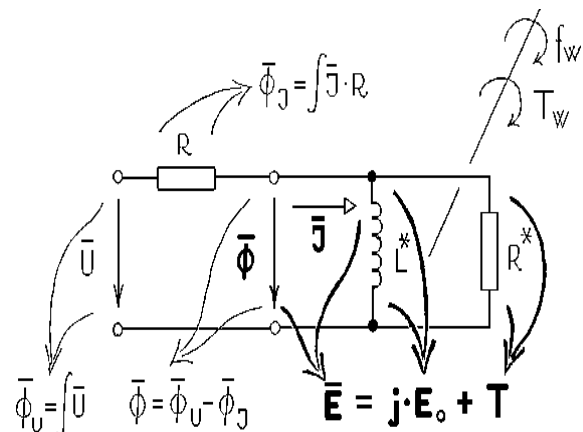


Fig. 1. Induction motor energy model

Determination of  $\bar{E}$  contact energy space vectors based on the relation between  $\bar{\phi}$  and  $\bar{I}$  space vectors

Determination of torque

As the result of the interaction of the directed fields represented by the  $\phi$  flux and the  $I_r$  rotor current,  $F^r$  rotor force is developed (see Fig. 2.). Similarly, the interaction of the directed fields,  $\phi$  and  $I_s$  develops the  $F^s$  stator force. Torque is developed as it is shown in Fig. 2. The torque can be determined by the following

equations.  $\vec{F}^r, \vec{F}^s, \vec{r}^r, \vec{r}^s$  are force and displacement vectors in the  $\vec{i}, \vec{j}, \vec{k}$  reference system.

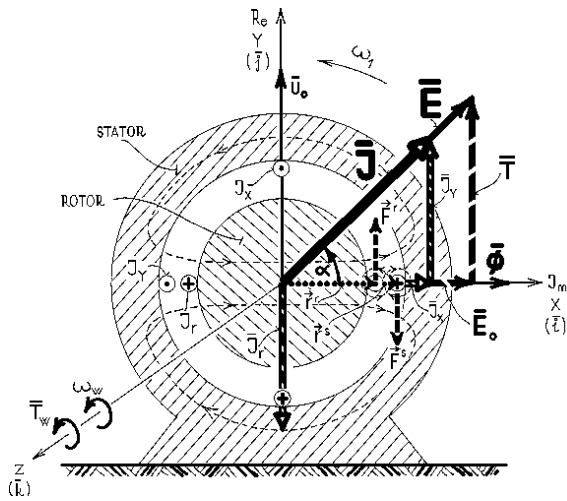


Fig. 2. Induction machine model with space vectors (operation as motor)

$$\vec{T}_w^s = \begin{vmatrix} \vec{i} & \vec{j} & \vec{k} \\ F_x^s & F_y^s & 0 \\ r_x^s & r_y^s & 0 \end{vmatrix} = \vec{k} \cdot (F_x^s \cdot r_y^s - F_y^s \cdot r_x^s) = \vec{k} \cdot T_w^s \text{ (Nm)}$$

$$\vec{T}_w^r = \begin{vmatrix} \vec{i} & \vec{j} & \vec{k} \\ r_x^r & r_y^r & 0 \\ F_x^r & F_y^r & 0 \end{vmatrix} = \vec{k} \cdot (r_x^r \cdot F_y^r - r_y^r \cdot F_x^r) = \vec{k} \cdot T_w^r \text{ (Nm)}$$

The mechanical degree of fields represented by  $\phi$  and  $I_r$  is equal to zero, therefore the resulting force is also equal to zero,  $\vec{T}_w^r = 0$ . If we take the mechanical degree of freedom of the system into consideration, the torque developed by the directed fields represented by the flux  $\phi$  and current  $I$  is given by the form:

$$\vec{T}_w = \begin{vmatrix} \vec{i} & \vec{j} & \vec{k} \\ \phi_x & \phi_y & 0 \\ I_x & I_y & 0 \end{vmatrix} = \vec{k} \cdot (\phi_x \cdot I_y - \phi_y \cdot I_x) = \vec{k} \cdot T_w \text{ (VAs), (Nm)}$$

Considering the degree of freedom, the next equation can be written:  $\vec{T}_w = \vec{T}_w^s$ .

Contact energy space vector

The following form can determine the Contact energy space vector:

$$\begin{aligned} \vec{E} &= (\vec{\phi} \cdot \vec{I}^*)^* \cdot j = \\ &= ((\phi_y + j \cdot \phi_x) \cdot (I_y - j \cdot I_x))^* \cdot j = \\ &= (\phi_x \cdot I_y - \phi_y \cdot I_x) + j \cdot (\phi_y \cdot I_y + \phi_x \cdot I_x) = \\ &= T + j \cdot E_0 \text{ (VAs)}. \end{aligned}$$

In this approach the potential effective energy ( $T$ ) is equal to the motor torque measured on the shaft of the machine ( $T_w$ ), i.e.  $T = T_w$ . The ( $E_0$ ) potential magnetic energy is equal to the energy represented by  $I_x$  (see Fig. 2.). It's value is constant (if  $I_x$  constant), but the spatial position of the directed field is changing.

Choosing Contact Energy and Current value

If the load angle  $\alpha = 45^\circ$ , choosing adequate gain,  $\vec{E} = \vec{T}$ , and  $|\vec{I}| = I$ . In order to determine the contact energy diagram for current  $I$ , the load angle  $\alpha$  have to be changed between  $-90^\circ$  and  $+90^\circ$ . In the followings the sign " " is neglected.

**3. COMBINED CONTACT ENERGY AND CONTACT ENERGY CONTROL DIAGRAM OF INDUCTION MACHINE**

The contact energy and contact energy control diagram of induction machine is shown in Fig. 3. The flux space vector is fixed to the real axes. The Contact energy

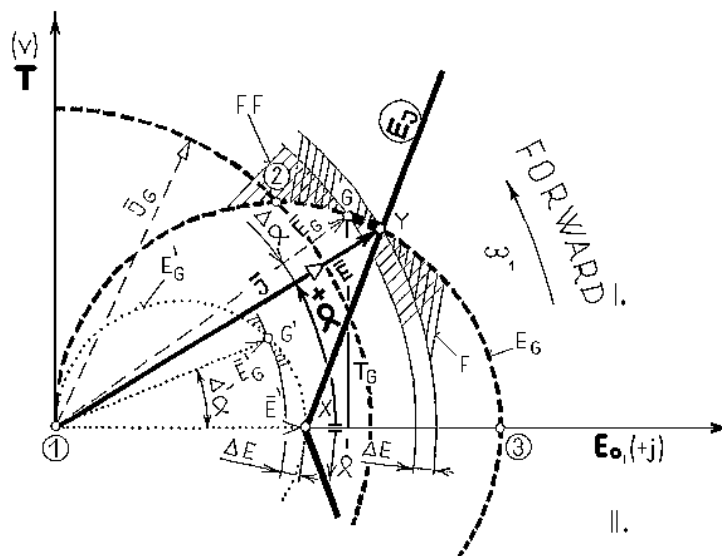


Fig. 3. Induction machine combined Contact Energy and Contact Energy Control diagram

diagram in the case of  $\bar{I}_G$  current limit is represented by broken line. The set points for this current value is determined by the  $\bar{I}$  and  $\bar{E}$  space vectors driven by thick line. If we determine the set points for every current value, the series of set points gives the Contact-Energy control diagram (continuous thick curved line). In order to obtain good adaptation for the technology process, the  $E_I$  contact energy reference value can be given by the equation:

$$E_I = \sqrt{2} \cdot I \cdot \sqrt{\left(\frac{B-A}{B-2A+I}\right)^Z}$$

Where:

- A : dc circuit current value at  $\alpha = 0^0$  load angle
- B : dc circuit current value at  $\alpha = 45^0$  load angle
- Z : transfer factor. A, B and Z are input parameters of the controller.

Z is usually equal to 1, but other values can also be chosen. The choice depends on the technology process.

In position 3 the total energy input is equal to the  $E_0$  component, and  $f_{rot} = 0$ .

In position 2,  $E_0 = T$  that is the breakdown torque value, and the rotor frequency is the breakdown value.

In position 1 ( $E_0 = T = 0$ ) the frequency has an infinite value.

The no-load point is signed by X. The controller works on the interval X-Y.  $\Delta E$  energy difference develops on the interval Y-G, that results frequency seeking and tracking. Other special positions on the diagram are:

F - FF : error surface,

$\omega_1$  : forward rotational direction,

I. : motor mode, forward,

II. : generator mode forward,

$\Delta\alpha, \Delta\alpha'$  : load angle difference,

$\bar{E}_G, \bar{E}_G'$  : contact energy with energy limit,

$T_G$  : torque limit.

#### 4. CONTACT ENERGY CONTROL – CURRENT BASED ENERGY CONTROL (CBEC)

The block diagram of the new controller is shown in Fig. 4. The scheme results fast and accurate control. After turning on the power supply, the controller immediately sets the mechanical speed. The controller gives good results at and around zero speed also.

The following control loops are used in the controller:

- 1 Energy controller, 2 Current controller, 3 Shaft-frequency controller, 4 Rotor-frequency controller.

The signals of the controller are:

- I dc current value,  $I_G$  dc circuit current limit value,  $\bar{I}$  current space vector,  $\bar{U}$  voltage space vector, R stator resistance,  $\alpha^*$  firing angle, U voltage reference value, N three-phase power network, E contact energy,  $E_I$  contact energy reference value,  $E_F$  contact energy error signal, A : dc circuit current value at  $\alpha = 0^0$  load angle, B : dc circuit current value at  $\alpha = 45^0$  load angle, Z : transfer factor,  $\Delta E$  contact energy difference, IT integrator inhibit,  $f_1$  stator frequency,  $f_2$  rotor frequency,  $f_w$  shaft frequency,  $f_{wo}$  shaft frequency reference value,  $f_\Delta$  frequency compensation, T effective energy,  $T_w$  shaft torque.

The main parts of the controller are:

- IFIMD Inverter-Fed Induction Motor Drive, EM Energy Model, ERU Energy Reference Unit, EC Energy Controller, CC Current Controller, SFSCU Shaft Frequency Seeking and Controlling Unit, RFI Rotor Frequency Interface.

#### 5. REALISATION OF THE CONTROLLER

The parts of the realised experimental current source inverter fed drive are shown in Fig. 5.

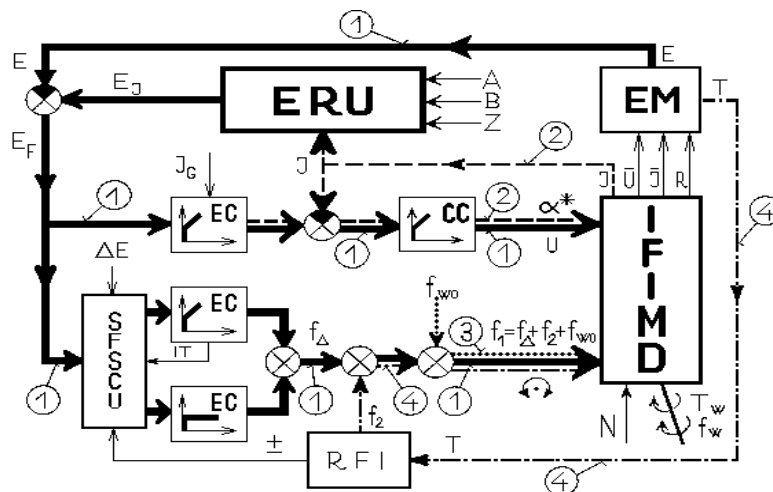


Fig. 4. Current based Energy Control (CBEC)

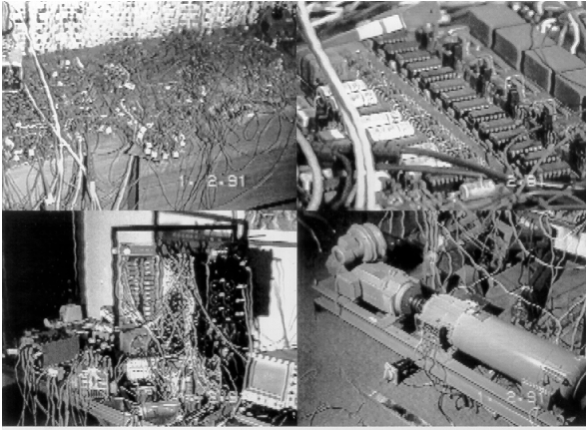


Fig. 5. The main parts of the experimental drive

Left upper picture: the parts of controller circuit, left lower picture: Thyristor rectifier and inverter, right upper picture: thyristor firing circuit, right lower picture: induction machine-dc machine used during the development work and tests.

## 6. EXPERIMENTAL RESULTS

The Oscilloscope signals of the experimental drives are shown in Fig. 6. and 7. The phase flux waveforms are displayed on the upper channels, while the phase current can be seen on the lower channels. The time scaling is 0.1s/division in Fig. 6. (The total time interval displayed on the screen is 1s).

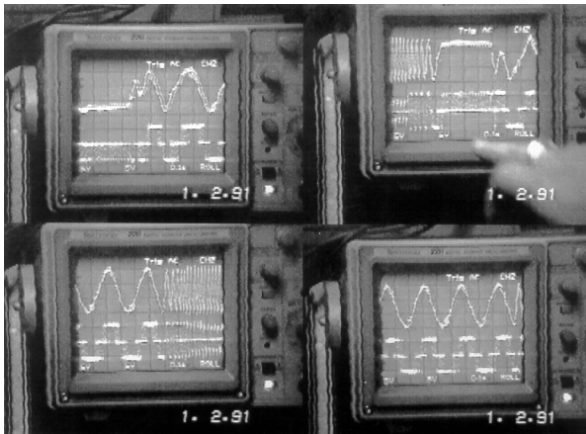


Fig. 6. Oscilloscope waveforms of the experimental drive

The scaling is 20ms/division in Fig. 7. During the measurements of waveforms Fig. 6. and Fig. 7. The induction motor was loaded by dc machine dynamically and forced it to change the speed and the rotational direction.

The zero and near zero speed behaviour and the phase current value produced by current pulses can be observe on the pictures. The resultant current field is swung forward and back automatically by the current based energy control (CBEC) strategy considering the dynamically changing demands of the load. In

consequence of the excellent dynamical behaviour of the drive, it is not possible to load the induction machine dynamically by the dc machine. (While Torque limit setting during the test:  $1.3 T_{rated}$  for the dc motor and  $T_{rated}$  for the induction motor). If the frequency of the reference signal of the ac drive is increased, the induction motor drive rotates forward and back with excellent dynamical behaviour.

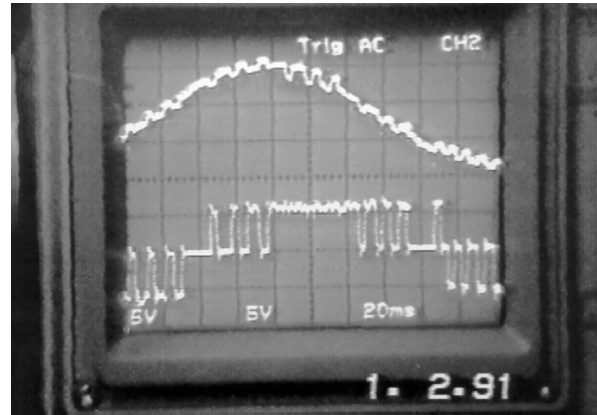


Fig. 7. Induction motor flux and current waveforms

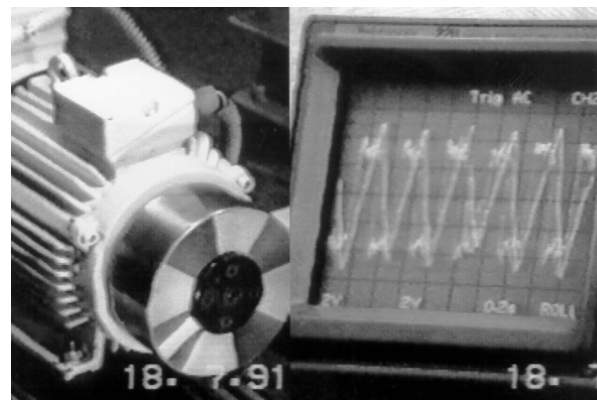


Fig. 8. Induction motor drive loaded by Balance wheel

Fig. 8. shows the induction motor loaded by balanced wheel. The drive is prepared for stroboscope test. The rotational lighted balance wheel is shown during the test measurement. The speed reference signal and the T component of the contact energy (torque) is displayed on the oscilloscope screen. The speed reference signal is changed forward and back in a random manner by hand.

## 7. CONCLUSIONS, SCIENTIFIC RESULTS

### Conclusions

The experimental tests show that the new sensor-less drive gives good results. The measurement or calculation of rotational speed can be neglected. The knowledge of the machine parameters is not necessary. The control strategy gives high precision and excellent dynamical behaviour. The machine is able to work on any set points with high stability. The self-control of the contact energy is realised (Direct self-control, DSC). The contact energy control can also be considered as current-based energy control

strategy (CBEC). with the new strategy. The contact energy control method is a new control strategy that can be used as general control strategy of converter-fed ac machine.

#### Scientific results

1. Recognition and application of E contact energy in induction machines.
2. Creation of contact energy diagram of induction machine. motor drives. Additionally, optimal energy transfer and easy fitting for technology process is possible
3. Development of the theory of contact energy control strategy, and contact energy control diagram.
4. Realisation and test of Current-based energy control (CBEC).
5. Future plan: optimisation of zero and very low speed control mode, applying the most up-to date technologies.

### 8. REFERENCES

- [1] Fekete, G.: Netzkommutierter Vektor - I - Umrichter. Europaeische Patentanmeldung EP 0 455 148 A2, 1991.
- [2] Fekete, G. - Szentirmai, L.: Revolving magnetic field in d - c chopper aided CSI-fed induction motor. Beijing International Symposium on Electromagnetic Field in Electrical Engineering, Beijing, China, 1988. Proceedings, Pergamen Press, pp: 75-78.
- [3] Fekete, G. - Szentirmai, L.: New performances of CSI-fed induction motor by field stepping of 30 degrees. International Conference on Electrical Machines, ICEM'88, Pisa, Italy, 1988. Proceedings, Vol. II. pp: 475-480.
- [4] Fekete, G. - Szentirmai, L.: Inverter and Converter Thyristors' Firing Control for CSI-Fed Induction Motor. European Conference on Power Electronics and Applications, EPE'85, Brussels, Belgium, 1985. Proceedings, Vol. 1. , pp: 835-838.
- [5] Fekete, G. - Szentirmai, L.: Advanced Inverter-Fed Induction Motor Drive: Neither Reactor nor Capacitor in D-C Link. Electric Energy Conference, EECON'87, An International Conference on Electrical Machines and Drives. Adelaide, 1987. The Institution of Engineers, Australia. Proceedings, pp: 718-723.
- [6] Fekete, G. - Niessen, E.: Energy Control of Induction Machines. Hungarian Patents pending. Hungarian Patent Office, Budapest. Reg. No. H 02 P 17/00 , P 94 01116, 1994.

### THE AUTHOR



**Dr Gabor Fekete:** Msc degree in Mechanical Engineering, 1974, University of Miskolc. Second degree in Electrical Control Engineering, 1983, Technical University of Budapest. Dr Univ. degree, 1985, University of Miskolc. Senior lecturer at the University of Miskolc. Five years Research work in BRD. Research fields are: Energy control of inverter fed drives, Energy theory.